



Glacial isostatic adjustment and nonstationary signals observed by GRACE

Paul Tregoning,¹ Guillaume Ramillien,^{2,3} Herbert McQueen,¹ and Dan Zwartz¹

Received 19 October 2008; revised 27 March 2009; accepted 28 April 2009; published 23 June 2009.

[1] Changes in hydrologic surface loads, glacier mass balance, and glacial isostatic adjustment (GIA) have been observed using data from the Gravity Recovery and Climate Experiment (GRACE) mission. In some cases, the estimates have been made by calculating a combination of the linear rate of change of the time series and periodic seasonal variations of GRACE estimates, yet the geophysical phenomena are often not stationary in nature or are dominated by other nonstationary signals. We investigate the variation in linear rate estimates that arise when selecting different time intervals of GRACE solutions and show that more accurate estimates of stationary signals such as GIA can be obtained after the removal of model-based hydrologic effects. We focus on North America, where numerical hydrological models exist, and East Antarctica, where such models are not readily available. The root mean square of vertical velocities in North America are reduced by $\sim 20\%$ in a comparison of GRACE- and GPS-derived uplift rates when the GRACE products are corrected for hydrological effects using the GLDAS model. The correlation between the rate estimates of the two techniques increases from 0.58 to 0.73. While acknowledging that the GLDAS model does not model all aspects of the hydrological cycle, it is sufficiently accurate to demonstrate the importance of accounting for hydrological effects before estimating linear trends from GRACE signals. We also show from a comparison of predicted GIA models and observed GPS uplift rates that the positive anomaly seen in Enderby Land, East Antarctica, is not a stationary signal related to GIA.

Citation: Tregoning, P., G. Ramillien, H. McQueen, and D. Zwartz (2009), Glacial isostatic adjustment and nonstationary signals observed by GRACE, *J. Geophys. Res.*, *114*, B06406, doi:10.1029/2008JB006161.

1. Introduction

[2] One aim of the Gravity Recovery and Climate Experiment (GRACE) mission [Tapley *et al.*, 2004] is to identify the gravity signal associated with glacial isostatic adjustment (GIA) of continental regions that were ice covered during the Last Glacial Maximum. Satellite altimetry and GRACE space missions detect not only the present-day mass change but also the remnant GIA signal. It is therefore not possible to estimate the component of present-day mass balance changes without first removing the GIA signal.

[3] On decadal timescales, GIA causes essentially linear changes in the geopotential over the affected regions. Thus attempts have been made to extract linear variations from existing GRACE solutions in order to estimate GIA signals [e.g., Tamisiea *et al.*, 2007]. In particular, a positive gravity rate anomaly seen in Enderby Land, East Antarctica [Chen

et al., 2006; Ramillien *et al.*, 2006; Lemoine *et al.*, 2007] has been interpreted as either an unmodeled GIA uplift or recent snow accumulation [Chen *et al.*, 2006] or, more recently, as reflecting errors in the GIA model or being related to snow accumulation [Chen *et al.*, 2008]. Despite this uncertainty in geophysical origin of the signals, linear rates are estimated from GRACE time series [e.g., Chen *et al.*, 2008].

[4] Hydrologic signals are typically cyclic in nature, with dominantly near-annual periods [Schmidt *et al.*, 2008]. Hydrologic processes cause significant variations in land surface heights and both good [e.g., Davis *et al.*, 2004] and poor [e.g., van Dam *et al.*, 2007] agreements have been found between estimates from GRACE and the Global Positioning System (GPS). However, interannual trends associated with, for example, droughts can cause multiyear increases/decreases and departures from simple periodic variations. If sufficiently large, such nonstationary variations (that is, variations that do not repeat in a regular, predictable pattern) in surface mass will be present in monthly GRACE solutions in addition to long-term, stable trends such as GIA. Global hydrological models such as GLDAS [Rodell *et al.*, 2004] have been used to model surface and soil moisture signals on broad scales [e.g., Syed *et al.*, 2008] and to mitigate the effects on GRACE estimates of GIA [Tamisiea *et al.*, 2007].

¹Research School of Earth Sciences, Australian National University, Canberra, ACT, Australia.

²Laboratoire d'Etudes en Géophysique et Océanographie, Centre Nationale de la Recherche Scientifique, Toulouse, France.

³Now at Dynamique Terrestre et Planétaire, Centre Nationale de la Recherche Scientifique, Toulouse, France.

[5] The aim of this paper is to demonstrate the nonstationary nature of many of the observed GRACE signals and to caution against the process of simply estimating a linear trend from monthly GRACE fields. We focus on two regions where the GIA signal is not well constrained by ice models (East Antarctica and Laurentia) and show that accurate secular trends can be estimated from GRACE after removing the dominant hydrologic signals, thereby permitting the long-term GIA signals to be identified. We also show from a combination of observed GPS uplift rates and predicted geoid rates from numerical models that the positive anomaly seen in Enderby Land is most likely not related to GIA.

[6] This paper is divided into three main parts. Firstly, we describe the GPS, GLDAS and GRACE data sets and relevant components of the analysis and utilization of the technique products. Next, we look in detail at the observed GIA signals in North America, a region covered by the GLDAS hydrology model, to demonstrate that a large portion of the observed GRACE signals are nonstationary and to highlight the importance of correcting for hydrologic effects before estimating linear rates from GRACE. Then, being mindful of the fact that hydrologic effects can affect significantly linear rate estimates from GRACE, we investigate the unexplained positive anomaly in Enderby Land, East Antarctica. Given that there is no available hydrologic model (such as GLDAS) that covers the Antarctic continent, we invoke different analytical techniques to distinguish between GIA and hydrological causes for the observed GRACE signals and conclude that the latter is more plausible.

2. Vertical Deformation From GRACE Observations

[7] The observed GRACE anomalies are a combination of components related to both elastic and viscoelastic effects, and the Stokes coefficients of the temporal spherical harmonic fields are the sum of the two effects.

$$\begin{pmatrix} \delta C_{nm}(t) \\ \delta S_{nm}(t) \end{pmatrix} = \begin{pmatrix} \delta C_{nm}^e(t) \\ \delta S_{nm}^e(t) \end{pmatrix} + \begin{pmatrix} \delta C_{nm}^v(t) \\ \delta S_{nm}^v(t) \end{pmatrix} \quad (1)$$

where n, m are the degree and order, $\delta C_{nm}, \delta S_{nm}$ are the Stokes coefficients of the GRACE anomaly fields at time t , and the superscripts e and v refer to the elastic and viscoelastic components, respectively. At monthly timescales, anomalies caused by surface loads can be considered to generate only elastic deformation. The elastic component of the anomalies observed by GRACE is [Wahr *et al.*, 1998]

$$\begin{pmatrix} \delta C_{nm}^e(t) \\ \delta S_{nm}^e(t) \end{pmatrix} = \frac{3\rho_w}{\rho_{av}} \frac{1+k'_n}{2n+1} \begin{pmatrix} \delta \hat{C}_{nm}(t) \\ \delta \hat{S}_{nm}(t) \end{pmatrix} \quad (2)$$

where ρ_w is the density of fresh water, ρ_{av} is the average density of the Earth, k'_n are elastic Love loading numbers [Pagiatakis, 1990] and $\delta \hat{C}_{nm}, \delta \hat{S}_{nm}$ are dimensionless Stokes coefficients that represent the surface load anomalies at time t . We can use the coefficients $\delta C_{nm}^e, \delta S_{nm}^e$ to calculate vertical elastic deformation [Davis *et al.*, 2004].

$$dU^e(\theta, \lambda, t) = R \sum_{n=0}^N \sum_{m=0}^n \frac{h'_n}{1+k'_n} \cdot P_{nm}(\cos\theta) (\delta C_{nm}^e(t) \cos m\lambda + \delta S_{nm}^e(t) \sin m\lambda) \quad (3)$$

where R is the mean radius of the Earth (6371 km), P_{nm} are the fully normalized Legendre functions and h'_n, k'_n are elastic Love loading numbers [Pagiatakis, 1990] computed for the Preliminary Reference Earth Model (PREM) [Dziewonski and Anderson, 1981].

[8] Long-term viscoelastic deformation associated with GIA can be approximated by [Wahr *et al.*, 2000]

$$dU^v(\theta, \lambda, t) = R \sum_{n=0}^N \sum_{m=0}^n \frac{2n+1}{2} \cdot P_{nm}(\cos\theta) (\delta C_{nm}^v(t) \cos m\lambda + \delta S_{nm}^v(t) \sin m\lambda) \quad (4)$$

where, in this case, $\delta C_{nm}^v, \delta S_{nm}^v$ are the coefficients representing the viscoelastic deformation components of the gravity changes observed by GRACE at time t . Thus in the elastic case, we multiply by $h'_n/(1+k'_n)$ whereas in the viscoelastic case we multiply by $(2n+1)/2$.

[9] It is not possible from the GRACE spherical harmonic fields alone to separate the elastic and viscoelastic components of the total Stokes coefficients. The surface load anomalies vary in an unpredictable manner with the changes in the hydrological cycles, hence are nonstationary in nature, whereas the viscoelastic signals associated with GIA will be essentially linear on timescales of years to decades.

3. Data

3.1. GPS

[10] It has been demonstrated that observations with the Global Positioning System (GPS) can detect GIA uplift patterns [e.g., Milne *et al.*, 2001; Lidberg *et al.*, 2007]. We analysed data from ~80 globally distributed GPS sites with the GAMIT/GLOBK software [Herring *et al.*, 2008] in a global analysis following, for example [Tregoning and Watson, 2009]. We used the VMF1 mapping function [Boehm and Schuh, 2004; Boehm *et al.*, 2006] with a priori zenith hydrostatic delays from ray-tracing through the ECMWF global weather model and we applied nontidal atmospheric pressure loading at the observation level. We transformed daily free-network solutions onto the terrestrial reference frame using ~30 globally distributed stabilization sites. We used coordinates for the stabilization sites from the ITRF2005, although we first removed a 1.8 mm/yr Z-translation velocity, being the difference between the ITRF2000 and ITRF2005 reference frames [Altamimi *et al.*, 2007]. This provides a reference frame with the internal consistency of the ITRF2005 (Z. Altamimi, personal communication, 2007) without the apparently geophysically implausible translation rate along the Z-axis [Argus, 2007].

[11] We estimated the GPS uplift rate at the Antarctic IGS sites at Mawson, Davis and our remote, solar-powered site at Richardson Lake in Enderby Land, East Antarctica as part of our global analysis (site locations are indicated on Figure 3). The latter site, affixed firmly to exposed bedrock, was installed in January 2007 specifically to estimate the present-day uplift rate in light of the positive gravity anomaly rate that had been identified in GRACE solutions [Chen *et al.*, 2006; Ramillien *et al.*, 2006]. To date, 153 days of data have been transmitted from the site by satellite communications, spanning 1.2 years.

[12] The most comprehensive estimate of vertical velocities in the North American region, from a combination of permanent and campaign-based observations, has been undertaken by *Sella et al.* [2007]. Their published velocities agree to within 1 mm/yr of our estimates at common sites (not shown); thus, we adopt their velocity estimates for the assessment of GRACE-derived GIA in North America (see section 5.1).

3.2. GRACE

[13] We used the monthly GRACE solutions from the Groupe de Recherche de Géodesie Spatiale as described by *Lemoine et al.* [2007]. These solutions use a 10-day sliding window approach to analyze the data in 30-day segments, with the first 10 days weighted by 0.25, the middle 10 days weighted by 0.5 and the last 10 days weighted by 0.25. An empirical constraint approach is used when estimating the spherical harmonic coefficients which negates the need to apply subsequent spatial filtering techniques. These solutions have been used previously to estimate, for example mass balance in Antarctica and Greenland [*Ramillien et al.*, 2006], co-seismic deformation [*Panet et al.*, 2007], hydrologic [e.g., *Ramillien et al.*, 2004] and oceanic signals [e.g., *Lombard et al.*, 2007; *Tregoning et al.*, 2008]. We calculated Stokes coefficient anomalies by subtracting the mean value over the time series 2002.6 to 2007.6 to derive values of δC_{nm} , δS_{nm} of equation (1).

3.3. Hydrology

[14] We used the GLDAS global hydrologic model [*Rodell et al.*, 2004] to generate estimates of changes in continental water mass, incorporating four soil moisture layers, accumulated snow quantity and total canopy storage. Previous studies have shown agreement between GRACE and GLDAS estimates of hydrologic signals [*Syed et al.*, 2008], although the GLDAS model does not include Antarctica nor valid modeling of Greenland [*Rodell et al.*, 2004]. Using the NOAH10 3-hourly values from 2002 to 2008, we computed the mean value at each 1° space grid node, then subtracted it from each 3-hourly field to generate anomaly values at each node (we set the anomaly values to zero over Greenland). We then generated monthly anomaly estimates at the epochs of the GRACE solutions, using the same weighting procedures invoked when the GRACE solutions are generated (see previous section). We converted these estimates into spherical harmonic coefficients, which are the $\delta \bar{C}_{nm}$, $\delta \bar{S}_{nm}$ coefficients of the right-hand side of equation (2), then converted them into elastic Stokes coefficients, δC_{nm}^e , δS_{nm}^e , using equation (2).

[15] The hydrology signals will affect the GRACE estimates of gravity change through the potential of the changing surface loads themselves and through the elastic deformation of the surface caused by the loads [e.g., *Wahr et al.*, 1998]. The latter effect will also affect the GPS estimate of station coordinates: since the GPS antennae are fixed to the surface of the Earth, they will detect any elastic deformation that might occur. We can thus utilise GPS coordinate estimate anomalies to validate the GLDAS model over the Laurentide region. The local deformation recorded by a GPS site will only be well modeled by the GLDAS model if the dominant signals are long wavelength; how-

ever, since the same is true of the relation between GRACE and hydrologic signals, it is an interesting comparison to make.

[16] We convolved the hydrology anomalies (in terms of equivalent water height) with elastic Greens functions [*Farrell*, 1972] using Load Love numbers from the PREM model and generated deformation anomalies using equations (2) and (3) (Figure 1). These agree well in phase with the GPS height anomalies at sites located around Churchill Bay in Canada, a region of significant GIA. The amplitude of the deformation from the GLDAS model underestimates the movement detected by GPS.

[17] We estimated the scale factor per site that would need to be applied to the GLDAS elastic deformations in order to match the GPS height anomalies and found that it varied considerably from site to site with a range from 1.1 to 2.7 (Figure 2). The differences may be caused by local hydrological phenomena that affect individual GPS sites but are not captured by the 1° space GLDAS model or deficiencies in the GLDAS model (which does not include all hydrological processes, e.g., groundwater), or perhaps errors in the ocean tide loading model (we used the FES2004 model) that alias to low-frequency signals. Lacking any better alternative, we used the GLDAS to model the hydrologic signals and assume that it captures the majority of the long-wavelength components in Canada. While this is not a perfect approach, the spatial variation in the scale factor estimates and the scarcity of permanent GPS sites in this region of Canada implies that we cannot verify whether modifying the GLDAS model through some spatially averaged scaling process would lead to a better result.

4. Linear Rate Estimates

[18] We first generated GRACE time series of vertical deformation, without removing the hydrologic component, to derive least squares estimates of linear rates and amplitudes/phases of annual periodic signals. This is the approach that has been used to study geoid rate signals [e.g., *Tamisiea et al.*, 2007; *Davis et al.*, 2008] as well as the GIA of Antarctica [e.g., *Chen et al.*, 2006, 2008]. Figure 3a shows the resulting linear trends obtained using the whole time series. Some particular significant features are immediately apparent, for example the mass loss occurring in West Antarctica [e.g., *Rignot et al.*, 2008] and southern Greenland [e.g., *Luthcke et al.*, 2006]. Other signals are either present when perhaps not expected (e.g., the positive signal in East Antarctica), are not clearly present or are not of the expected magnitude (e.g., the GIA signals in North America and Fennoscandia).

[19] We next considered rate estimates using subsets of the total GRACE data to investigate the spatial stability of the observed signals. We first separated the time series into two, utilizing 3 years of data for each estimate. Figures 3b and 3c show the rate field for 2002.6–2005.6 and 2004.6–2007.6, respectively. A comparison of these fields shows that some of the signals seen in Figure 3a are always present, indicating the stationary nature of the signal. The mass loss in West Antarctica decreases slightly in magnitude while there is a $\sim 50\%$ increase in mass loss in southeast Greenland. The mass loss in southern Alaska appears to

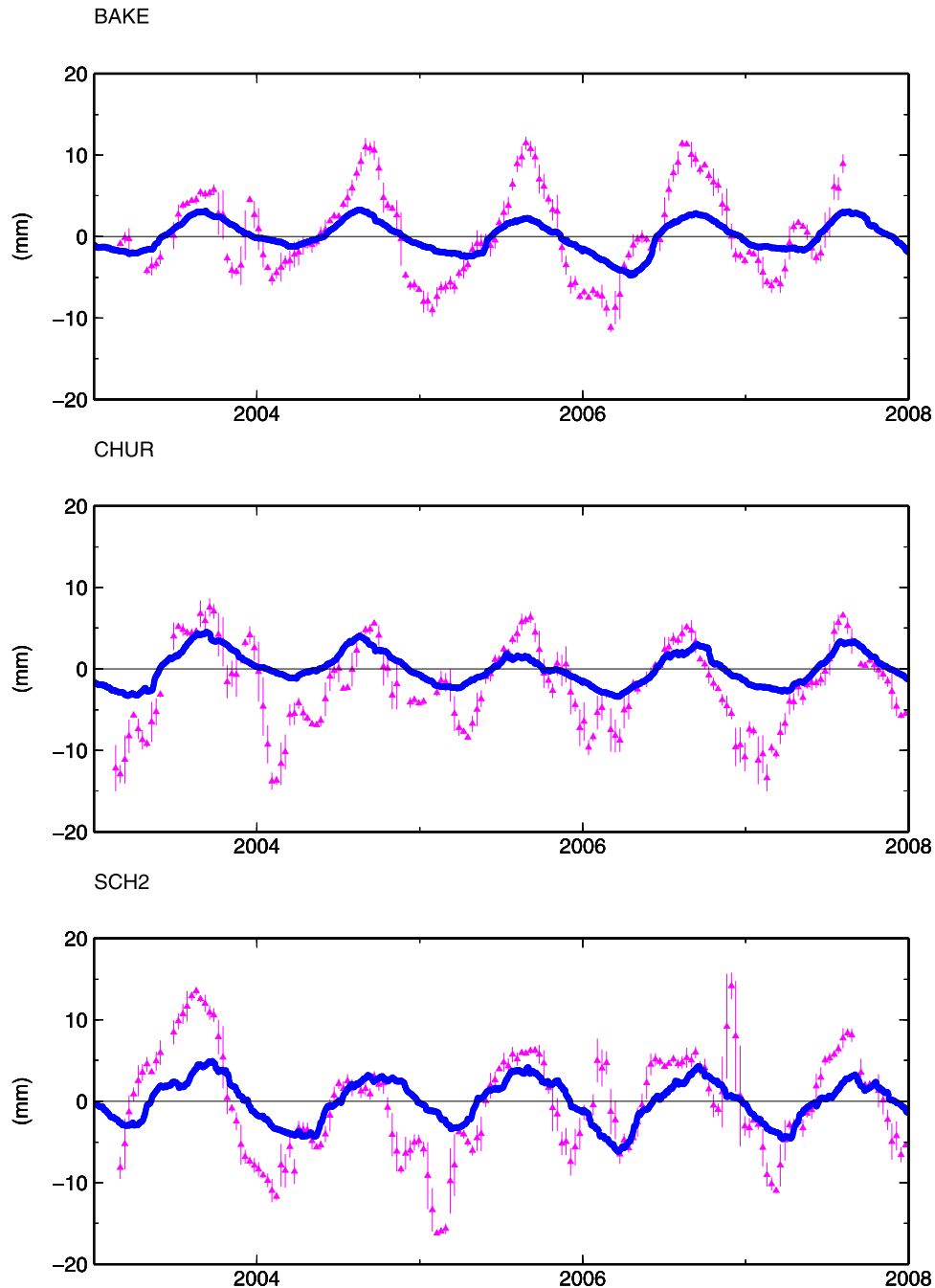


Figure 1. Comparison of residual height variations estimated from GPS (pink) and calculated by convolving GLDAS hydrologic anomalies into elastic vertical deformation (blue) at GPS sites Baker Lake (BAKE), Churchill Bay (CHUR), and Scherrerville (SCH2), all in eastern Canada (see Figure 2).

have decelerated, while mass loss may have commenced in northwestern Greenland to the south of Thule. Many of these features are either not visible or are significantly damped in the rate estimates from the whole time series. These are the geophysical interpretations that could be made, but we are not suggesting that these are valid interpretations since seasonal hydrological signals still remain in these GRACE results.

[20] To separate the stationary, viscoelastic effects from the nonstationary, hydrologic effects, we subtracted from

the monthly GRACE spherical harmonic anomaly coefficients (δC_{nm} , δS_{nm}) the monthly GLDAS coefficients (i.e., the $\delta C_{nm}^e(t)$, $\delta S_{nm}^e(t)$ terms of equation (1)), making the assumption that the hydrological signals captured by the GLDAS model will account for all elastic-related surface mass variations detected by GRACE. The remaining signals should be related mainly to the nonelastic processes of GIA, but will also include any unmodeled hydrological or oceanic elastic signals. We can then generate trend estimates from time series of values for each 10-day epoch on a global grid

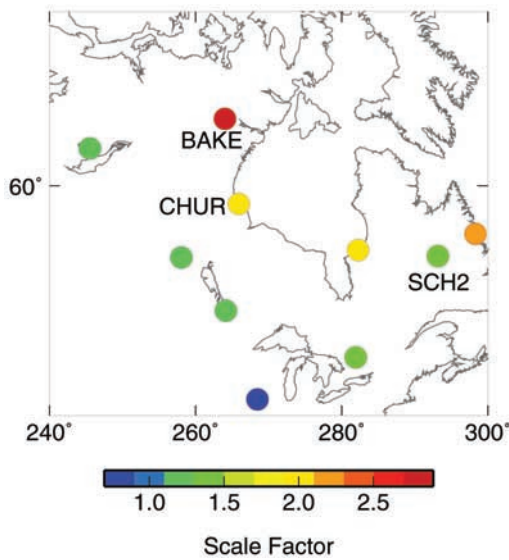


Figure 2. Scale factor estimates at GPS sites in North America between observed GPS height anomalies and elastic deformation calculations using water load anomalies from the GLDAS model.

using equation (4), thus deriving viscoelastic vertical deformation as observed by GRACE. This approach is more rigorous than that of *Tamisiea et al.* [2007] who removed the effects of hydrological changes when computing free-air gravity trends over northern Canada by subtracting from the GRACE trends a trend estimated from GLDAS data (one does not obtain the same velocity estimate from (1) estimating a velocity from raw GPS heights, separately from GLDAS vertical elastic deformation computations and differencing the velocities; and (2) correcting the GPS heights for the GLDAS-derived elastic deformation, then using the corrected time series to estimate the velocity). Figure 4 shows time series of the original GRACE solutions, the GLDAS elastic deformation predictions and GRACE minus GLDAS at Flin Flon in southern Canada (54.7°N, 258.0°E). By propagating the formal uncertainties of the GRGS monthly GRACE fields, we calculated that the uncertainty of each monthly estimate of vertical position anomaly is around 15–25 mm (Figure 4), leading to a formal uncertainty of the rate estimates of ~1 mm/yr. We consider this to be an optimistic estimate of the uncertainty since it does not include any estimate of error in the GLDAS fields. We acknowledge also that any errors in the GLDAS representation of the hydrological effects will still remain in our uplift rate estimates; however, there is not currently a superior approach available to that which we have used here.

5. Discussion

5.1. Laurentia

[21] GIA models for North America predict significant vertical uplift rates, with the magnitude depending on the choice of ice history and viscosity models [e.g., *Peltier, 2004*]. Numerous studies have observed uplift from GPS data [e.g., *Calais et al., 2006; Sella et al., 2007*] and tide

gauge observations [e.g., *Snay et al., 2007*] as well as the free-air gravity signal from GRACE observations [*Tamisiea et al., 2007*]. The predicted uplift signal over Laurentia computed from GRACE solutions (2002.6–2007.6) when ignoring the possible presence of elastic effects is shown in Figure 5a. Three positive uplift regions are visible, along with a zone of subsidence around (E250° space N59°). In

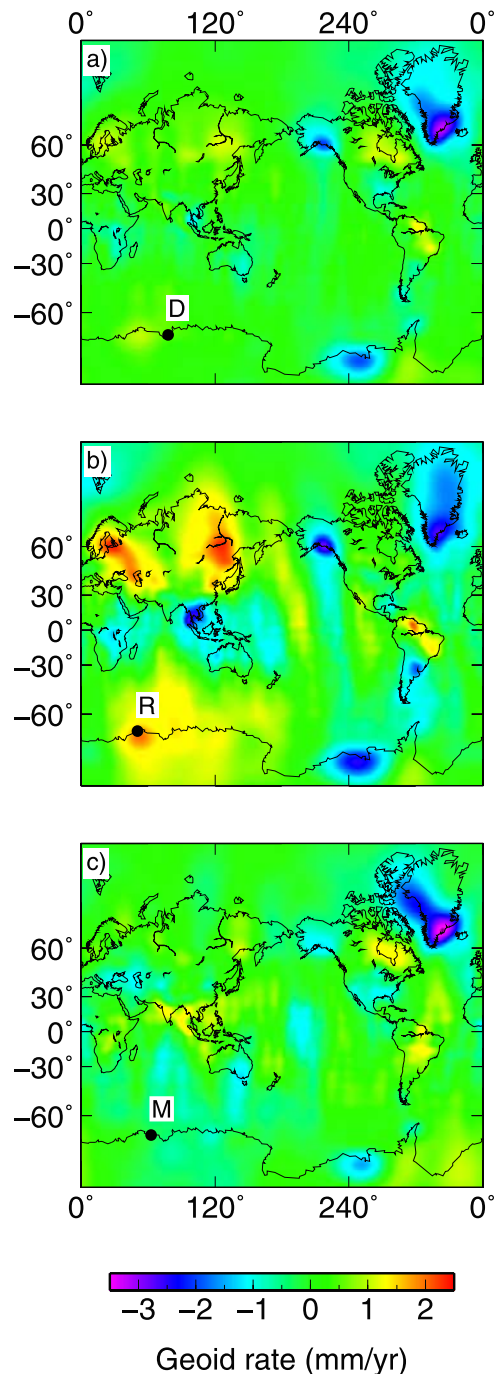


Figure 3. Linear trend estimates (in terms of geoid rate) using GRACE solutions spanning (a) 2002.6 to 2007.6, (b) 2002.6 to 2005.6, and (c) 2004.6 to 2007.6. GPS sites in Antarctica are indicated as D for Davis, M for Mawson, and R for Richardson Lake.

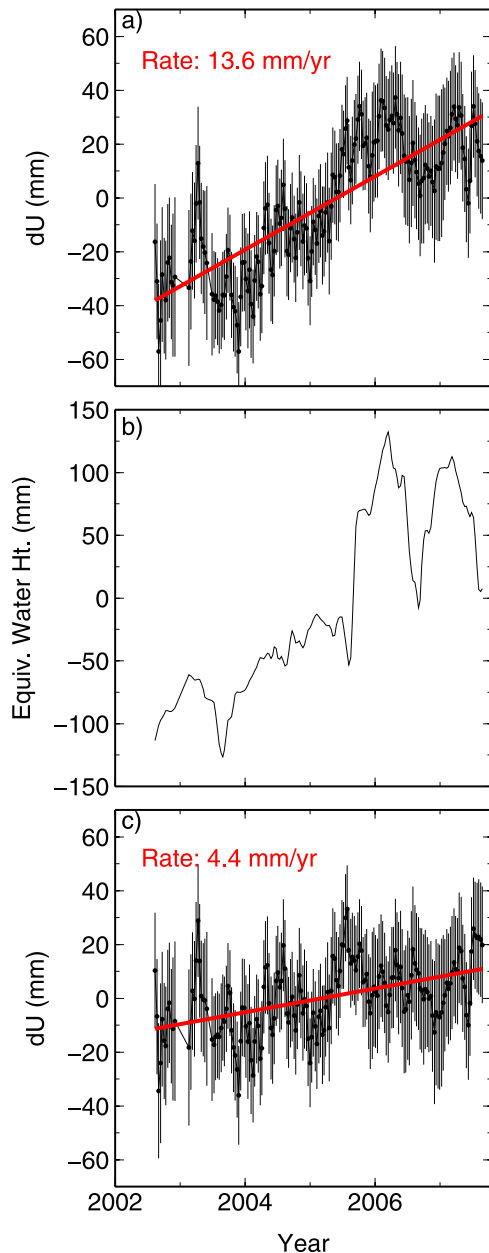


Figure 4. (a) Time series of surface height (in terms of vertical viscoelastic deformation) at 54.7° , 258.0° E, using GRACE-only solutions. (b) Time series of GLDAS anomalies, expressed in terms of equivalent water height. (c) As for Figure 4a but with the nonstationary hydrological signals removed using the GLDAS model.

general, the pattern does not correspond well with that predicted from GIA models [e.g., *Peltier*, 2004].

[22] Interannual hydrologic variations that occur in North America create nonstationary signals in the GRACE observations, which contaminate the purely stationary GIA signals. Accounting first for the hydrological signals in the GRACE spherical harmonic anomalies, then estimating the linear trends yields a significantly different result (Figure 5b). The positive zone around (54° N, 260° E) is reduced in magnitude while the zone of subsidence at 250° E

is eliminated completely. Neither of these signals feature in GIA models for Laurentia and are not related to the GIA processes. The negative signal below 50° N at around 260° E is more likely to be remaining hydrologic signal not captured by GLDAS than to be related to a peripheral bulge signal of GIA.

[23] The uplift pattern of the ICE-5G (VM2) model has three notable centers of maximum uplift, associated with the three primary ice dome complexes in that model: one over Keewatin near Yellowknife, one in southeast Hudson Bay, and the third in the Foxe Basin to the west of Baffin Island [*Peltier*, 2004, Figure 21]. Our uplift estimates show clearly the first two regions but, because the hydrology of Greenland is poorly represented in the GLDAS model [*Rodell et al.*, 2004], we do not show on Figure 5 nor discuss here the third center.

[24] The pattern of uplift west of Hudson Bay has a maximum of ~ 12 mm/yr and is slightly elongated in an E-W direction. There are a number of interesting features of this center: firstly, there is a clear separation between this maximum and that of the center to the southeast of Hudson Bay. Secondly, the extension of the region toward Yellowknife is supportive of substantial ice loss in this region. Available shoreline data in the Canadian region cannot provide constraints on the likely thickness of the ice shield in this region at the Last Glacial Maximum (LGM) (K. Lambeck, personal communication, 2008), nor are there any GPS sites in the vicinity from which to estimate directly the ongoing uplift. Thus this estimate from GRACE solutions provides new spatial observations of present-day signals. The shape of the pattern is in general agreement with the hydrology-corrected free-air gravity anomaly map of *Tamisiea et al.* [2007]. A clear positive region appears southeast of Hudson Bay, corresponding with the location of a dome in the ICE-5G (VM2) model [*Peltier*, 2004, Figure 21] but with a larger amplitude (~ 17 mm/yr compared with ~ 14 mm/yr). This zone of uplift is also present in the models of *Lambeck et al.* [2008].

[25] Predictions of uplift rate from GIA models are dependent on both the ice history and viscosity models used; therefore, the usefulness of a comparison of GRACE-derived and GIA model-derived uplift rates is limited by the accuracy of each of the models, where the true accuracy of each is unknown. We compare our GRACE-derived velocities with GPS-derived uplift rates of *Sella et al.* [2007] covering the region. The latter estimates are independent of ice model and viscosity and so provide a better alternative for assessing the accuracy of the two GRACE models. The RMS differences between our GRACE velocity fields and the GPS uplift rates are 3.7 mm/yr and 3.0 mm/yr for GRACE-only and GRACE-GLDAS, respectively, showing a $\sim 20\%$ improvement in agreement with the GPS velocities once the hydrologic signals are removed. There is also an improvement in the correlation between the GPS and GRACE velocities (0.58 for GRACE-only, 0.73 for GRACE-GLDAS) (Figures 5b and 5d). A similar pattern of uplift rates has recently been found by *van der Wal et al.* [2008] in a study of GIA in North America.

5.2. Enderby Land, Antarctica

[26] The above investigation demonstrates that not accounting for nonstationary hydrological effects can signif-

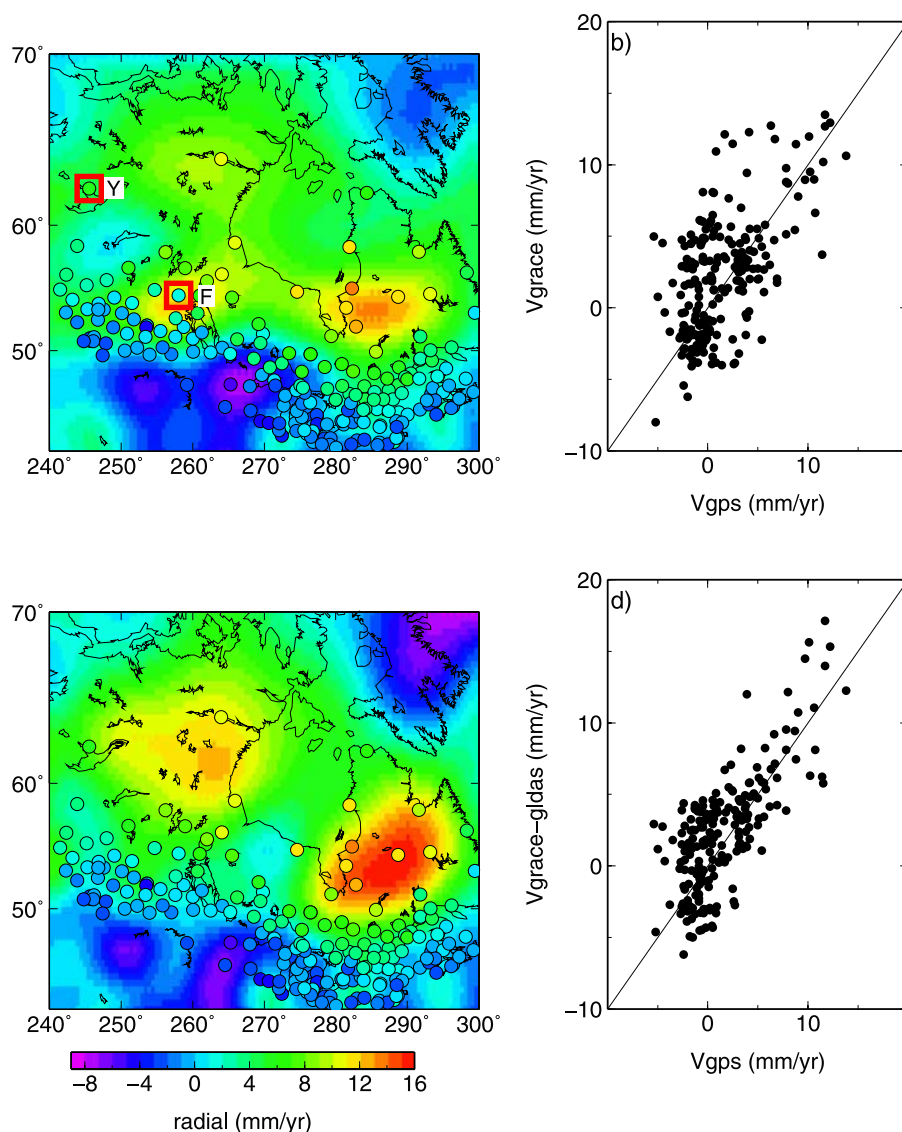


Figure 5. (a) Uplift rates from GRACE for the Laurentide region including hydrologic signals and (c) with hydrologic signals removed. Vertical velocities estimated from GPS observations by *Sella et al.* [2007] are shown using the same color scheme. (b) Comparison of GRACE-derived and GPS uplift velocities including hydrologic signals and (d) with the GLDAS model removed from each monthly field. The locations of Yellowknife (Y) and Flin Flon (F) are indicated (red squares) in Figure 5a.

icantly bias the linear rate estimates of GIA. Despite any possible shortcomings of the GLDAS model, the fact that such models exist at all for North America make such studies possible. On the other hand, no such models are publicly available that cover the Antarctic continent so the same approach cannot be used to obtain the GIA estimates from GRACE over Antarctica. In this section we invoke a different approach to study positive anomaly signals which have been detected in Enderby Land, East Antarctica. We compare viscoelastic modelling and a comparison with GPS-derived uplift rates to assess whether GIA or interannual snow accumulation are the most likely cause of the signals observed by GRACE.

[27] *Chen et al.* [2008] estimated a rate of change of 33.7 ± 0.65 mm/yr of equivalent water height in the center of the positive anomaly feature in Enderby Land, confirming the

earlier detection of a positive anomaly in this region [*Chen et al.*, 2006; *Ramillien et al.*, 2006]. Figure 6 shows (in red) a time series at this location (point D in Figure 7a) from the GRGS GRACE solutions. This is comparable to the time series shown by *Chen et al.* [2008, Figure 5b] except that we express the gravity field changes as vertical deformation rather than surface load in terms of equivalent water height. Estimating the uplift rate from the last three rather than the first three years of the total time series changes the rate estimate from 19.3 ± 2.3 mm/yr to 2.5 ± 2.1 mm/yr, with an average rate over the entire series of 10.3 ± 1.1 mm/yr (Figure 6). The rates are not constant, indicating that the time series is dominated by a signal(s) other than linear GIA. Possible interpretations of the time series are that no significant GIA is occurring (the variations in the time series are related to variations in accumulated snow/ice) or that

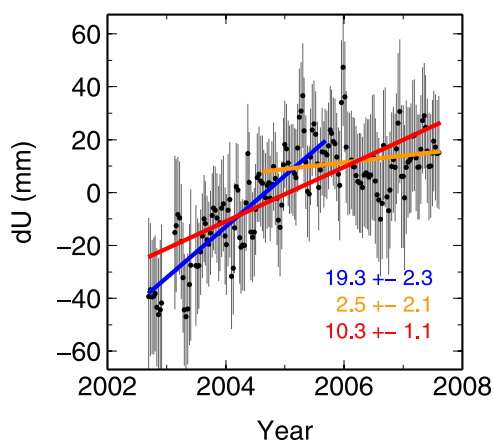


Figure 6. Time series of gravity variations (expressed as vertical deformation using equation (4)) at point D in Figure 7a. Uplift rates (in mm/yr) shown are estimated from the first three years (blue), the last three years (orange), and the entire time series (red).

destructive interference has occurred in the latter part of the time series between an underlying uplift signal and significant hydrologic mass loss.

[28] Because we can't remove the hydrology signals, we instead simulated an ice load over the region using a viscoelastic earth model with 65 km lithospheric thickness, upper mantle viscosity of 4×10^{20} Pa s and lower mantle viscosity of 10^{22} Pa s [Lambeck *et al.*, 1998] to generate a geoid rate anomaly comparable to that seen in the GRACE solutions.

[29] The choice of a larger lithospheric thickness would reduce the high-frequency component of the modeled GIA signal and may affect the conclusions; however, the value used is typical of values used in other studies [e.g., *Ivins and James*, 2005]. There is not a unique solution to this forward modelling process: a model with more ice loss earlier will generate a similar present-day signal to a model with less ice loss more recently. Therefore we attempted to cover the range of possibilities by generating simulated geoid rate patterns for two models, one with ice loss of a 1200 m cylinder occurring linearly between 11 ka and 3.5 ka (the time interval of Antarctic ice melt in the ICE-5G model [Peltier, 2004]) (Figure 7b) and the other with 600 m ice loss occurring between 3.5 ka and 1 ka (Figure 7c). We stress that there are not currently any geophysical observations to support the presence of such ice quantities in the past; this is simply an exercise to develop a GIA model that can reproduce the positive geoid rate anomaly seen by GRACE in Enderby Land.

[30] Figures 7d and 7e show the present-day vertical deformation associated with each of the models, with predicted uplift rates of ~ 10 mm/yr at RICH and MAW1. The uplift rates at these sites estimated from GPS observations are near zero and statistically significantly different from the predicted rates at the 99% confidence level (Figure 8). While, admittedly, the time series at RICH spans only 1.2 years, the height estimates clearly do not align with the predicted rate (red line in Figure 8c). In other words, it is not likely that a GIA model can generate a positive gravity anomaly that matches the Enderby Land feature and, simultaneously,

matches the GPS-observed surface uplift rates. This arises because one cannot have a geoid rate signal without having an associated uplift of the continental surface.

6. Conclusions

[31] Nonstationary hydrologic signals distort estimates of long-term GIA from GRACE data if a linear rate is estimated through uncorrected GRACE fields. Removing the signals using a global hydrologic model enables the extraction of stationary, linear signals, which are more consistent with ground-based estimates of vertical uplift

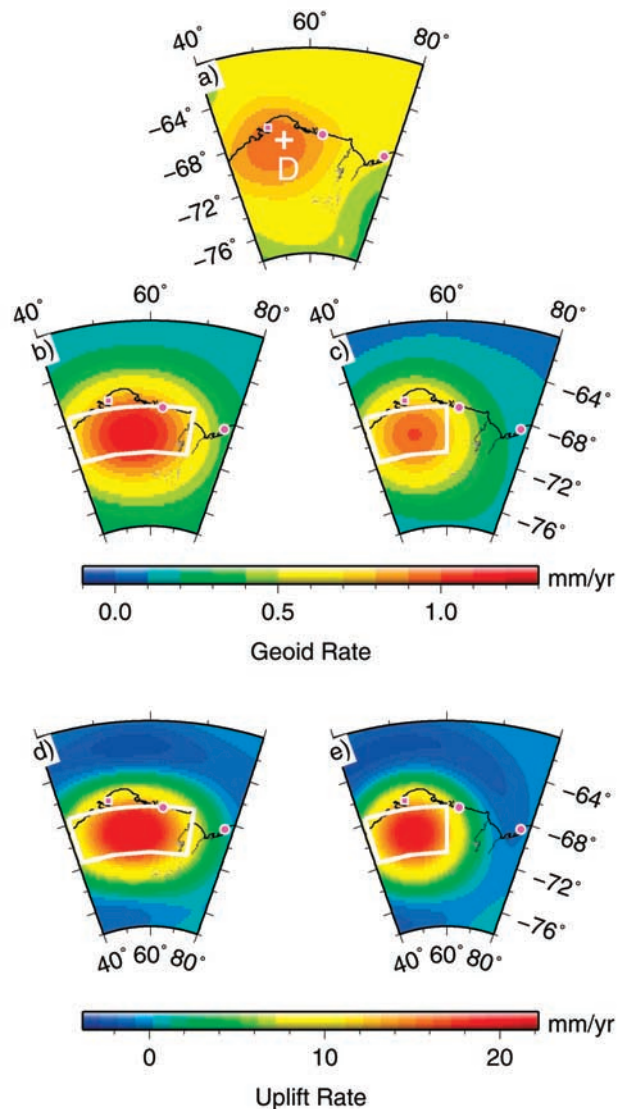


Figure 7. (a) GRACE geoid rate over Enderby Land, East Antarctica. The cross labeled D ($S68^\circ$, $E54^\circ$) indicates the approximate location used by *Chen et al.* [2008] to compute the linear trend in Figure 6. Geoid rates associated with (b) 1200-m ice loss from 11 ka to 3.5 ka and (c) 600-m ice loss from 3.5 ka to 1 ka. (d) Present-day vertical velocities associated with Figure 7b and (e) associated with Figure 7c. The locations of the nearest GPS sites are shown, whereas the white outlines show the spatial extents of the regions where extra ice has been melted.

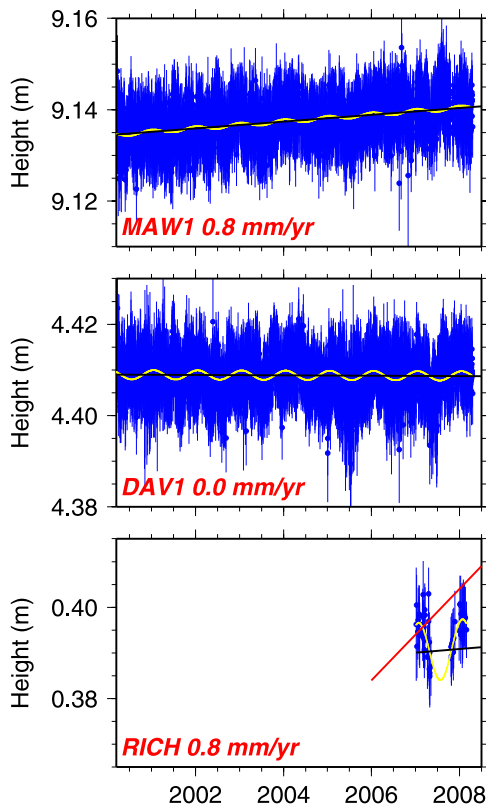


Figure 8. GPS height time series at (a) Mawson (MAW1), (b) Davis (DAV1), and (c) Richardson Lake (RICH) in Antarctica. The yellow lines are the modeled values of a rate and annual term, the black lines show the rate only. The red line in Figure 8c represents the 10 mm/yr uplift rate predicted by the GIA models that approximate the observed geoid signal seen by GRACE.

rates. The GRACE-derived uplift pattern in the Laurentide region provides spatial information on the GIA process in regions that lie between GPS sites and also where the available geomorphological and shoreline observations cannot constrain the ice thicknesses during the last glacial period. Such GRACE estimates provide important additional constraints in inversions of geological and geophysical data to construct a more accurate ice model for North America.

[32] The positive anomaly in Enderby Land identified in other studies [Chen *et al.*, 2006; Ramillien *et al.*, 2006; Chen *et al.*, 2008] is not a GIA signal that has been overlooked in recent GIA models for Antarctica (ICE-5G [Peltier, 2004], IJ05 [Ivins and James, 2005]): GPS uplift rates estimated both in Enderby Land and at Mawson and Davis are incompatible with the predicted uplift rates associated with ice loss models implied by the geoid rate signal seen in the region. Thus we attribute the cause of the positive anomaly in Enderby Land to the accumulation of snow over the 2002–2005 period. The recent GRACE solutions indicate a relatively constant mass since 2005.

[33] **Acknowledgments.** We thank the GRGS GRACE team for making their solutions freely available and the IGS for the global GPS data. The GPS fieldwork undertaken in Enderby Land was supported by the Australian Antarctic Division and we thank the many field, station, and

logistics personnel who contributed to the fieldwork. We thank K. Lambeck and T. Purcell for the use of their GIA modeling software. The GPS data were computed on the Terrawulf II computational facility at the Research School of Earth Sciences, a facility supported through the AuScope initiative. AuScope Ltd. is funded under the National Collaborative Research Infrastructure Strategy (NCRIS), an Australian Commonwealth Government Programme. We thank the associate editor and three anonymous reviewers whose helpful review comments improved this manuscript.

References

- Altamimi, Z., X. Collilieux, J. Legrand, B. Garayt, and C. Boucher (2007), ITRF2005: A new release of the International Terrestrial Reference Frame based on time series of station positions and Earth orientation parameters, *J. Geophys. Res.*, *112*, B09401, doi:10.1029/2007JB004949.
- Argus, D. (2007), Defining the translational velocity of the reference frame of Earth, *Geophys. J. Int.*, *169*, 830–838.
- Boehm, J., and H. Schuh (2004), Vienna mapping functions in VLBI analyses, *Geophys. Res. Lett.*, *31*(1), L01603, doi:10.1029/2003GL018984.
- Boehm, J., B. Werl, and H. Schuh (2006), Troposphere mapping functions for GPS and very long baseline interferometry from European Centre for Medium-Range Weather Forecasts operational analysis data, *J. Geophys. Res.*, *111*, B02406, doi:10.1029/2005JB003629.
- Calais, E., J. Y. Han, C. DeMets, and J. M. Nocquet (2006), Deformation of the North American plate interior from a decade of continuous GPS measurements, *J. Geophys. Res.*, *111*, B06402, doi:10.1029/2005JB004253.
- Chen, J. L., C. R. Wilson, D. D. Blankenship, and B. D. Tapley (2006), Antarctic mass rates from GRACE, *Geophys. Res. Lett.*, *33*, L11502, doi:10.1029/2006GL026369.
- Chen, J. L., C. R. Wilson, B. D. Tapley, D. Blankenship, and D. Young (2008), Antarctic regional ice loss rates from GRACE, *Earth Planet. Sci. Lett.*, *266*, 140–148.
- Davis, J. L., P. Elósegui, J. X. Mitrovica, and M. E. Tamisiea (2004), Climate-driven deformation of the solid Earth from GRACE and GPS, *Geophys. Res. Lett.*, *31*, L24605, doi:10.1029/2004GL021435.
- Davis, J. L., M. E. Tamisiea, P. Elósegui, J. X. Mitrovica, and E. M. Hill (2008), A statistical filtering approach for Gravity Recovery and Climate Experiment (GRACE) gravity data, *J. Geophys. Res.*, *113*, B04410, doi:10.1029/2007JB005043.
- Dziewonski, A. M., and D. L. Anderson (1981), Preliminary reference Earth model, *Phys. Earth Planet. Inter.*, *25*, 297–356.
- Farrell, W. E. (1972), Deformation of the Earth by surface loads, *Rev. Geophys.*, *10*, 761–797.
- Herring, T. A., R. W. King, and S. McClusky (2008), *Introduction to GAMIT/GLOBK*, Mass. Inst. of Technol., Cambridge, Mass.
- Ivins, E., and T. James (2005), Antarctic glacial isostatic adjustment: A new assessment, *Antarct. Sci.*, *17*, 541–553, doi:10.1017/S0954102005002968.
- Lambeck, K., C. Smither, and P. Johnston (1998), Sea-level change, glacial rebound and mantle viscosity for northern Europe, *Geophys. J. Int.*, *134*, 102–144.
- Lambeck, K., T. Purcell, and J. Zhao (2008), Sea levels and ice sheets during the last glacial cycle: New results from glacial rebound modelling, paper presented at Geological Society William Smith 2008 Meeting, Observations and Causes of Sea-Level Changes on Millennial to Decadal Timescales, London, U. K., 1–2 Sept.
- Lemoine, J.-M., S. Bruinsma, S. Loyer, R. Biancale, J.-C. Marty, F. Perosanz, and G. Balmino (2007), Temporal gravity field models inferred from GRACE data, *Adv. Space Res.*, *39*, 1620–1629.
- Lidberg, M., J. M. Johansson, H.-G. Sclerneck, and J. L. Davis (2007), An improved and extended GPS-derived 3D velocity field of the glacial isostatic adjustment (GIA) in Fennoscandia, *J. Geod.*, *81*, 213–230.
- Lombard, A., D. Garcia, G. Ramillien, A. Cazenave, R. Biancale, J.-M. Lemoine, F. Flechtner, R. Schmidt, and M. Iishi (2007), Estimation of steric sea level variations from combined GRACE and Jason-1 data, *Earth Planet. Sci. Lett.*, *254*, 194–202.
- Luthcke, S. B., H. J. Zwally, W. Abdalati, D. D. Rowlands, R. D. Ray, R. S. Nerem, F. G. Lemoine, J. J. McCarthy, and D. S. Chinn (2006), Recent Greenland ice mass loss by drainage system from satellite gravity observations, *Science*, *314*, 1286–1289, doi:10.1126/science.1130776.
- Milne, G. A., J. L. Davis, J. X. Mitrovica, H.-G. Sclerneck, J. M. Johansson, M. Vermeer, and H. Koivula (2001), Space-geodetic constraints on glacial isostatic adjustment in Fennoscandia, *Science*, *291*, 2381–2385.
- Pagiatakis, S. D. (1990), The response of a realistic earth to ocean tide loading, *Geophys. J. Int.*, *103*, 541–560.
- Panet, I., V. Mikhailov, M. Diament, F. Pollitz, G. King, O. de Viron, M. Holschneider, R. Biancale, and J.-M. Lemoine (2007), Coseismic and post-seismic signatures of the Sumatra 2004 December and 2005 March earthquakes in GRACE satellite gravity, *Geophys. J. Int.*, *171*, 177–190.

- Peltier, W. R. (2004), Global glacial isostasy and the surface of the ice-age Earth: The ICE-5G (VM2) model and GRACE, *Annu. Rev. Earth Planet. Sci.*, *32*, 111–149.
- Ramillien, G., A. Cazenave, and O. Brunau (2004), Global time variations of hydrological signals from GRACE satellite gravimetry, *Geophys. J. Int.*, *158*(3), 813–826.
- Ramillien, G., A. Lombard, A. Cazenave, E. R. Ivins, M. Llubes, F. Remya, and R. Biancale (2006), Interannual variations of the mass balance of the Antarctica and Greenland ice sheets from GRACE, *Global Planet. Change*, *53*, 198–208.
- Rignot, E., J. L. Bamber, M. R. van den Broeke, C. Davis, Y. Li, W. Jan van de Berg, and E. van Meijgaard (2008), Recent Antarctic ice mass loss from radar interferometry and regional climate modelling, *Nat. Geosci.*, *1*, 106–110, doi:10.1038/ngeo102.
- Rodell, M., et al. (2004), The global land data assimilation system, *Bull. Am. Meteorol. Soc.*, *85*, 381–394.
- Schmidt, R., S. Petrovic, A. Güntner, F. Barthelmes, J. Wunsch, and J. Kusche (2008), Periodic components of water storage changes from GRACE and global hydrology models, *J. Geophys. Res.*, *113*, B08419, doi:10.1029/2007JB005363.
- Sella, G. F., S. Stein, T. H. Dixon, M. Craymer, T. S. James, S. Mazzotti, and R. K. Dokka (2007), Observation of glacial isostatic adjustment in “stable” North America with GPS, *Geophys. Res. Lett.*, *34*, L02306, doi:10.1029/2006GL027081.
- Snay, R., M. Cline, W. Dillinger, R. Foote, S. Hilla, W. Kass, J. Ray, J. Rohde, G. Sella, and T. Soler (2007), Using global positioning system-derived crustal velocities to estimate rates of absolute sea level change from North American tide gauge records, *J. Geophys. Res.*, *112*, B04409, doi:10.1029/2006JB004606.
- Syed, T. H., J. S. Famiglietti, M. Rodell, J. Chen, and C. R. Wilson (2008), Analysis of terrestrial water storage changes from GRACE and GLDAS, *Water Resour. Res.*, *44*, W02433, doi:10.1029/2006WR005779.
- Tamisica, M. E., J. X. Mitrovica, and J. L. Davis (2007), GRACE gravity data constrain ancient ice geometries and continental dynamics over Laurentia, *Science*, *316*, 881, doi:10.1126/science.1137157.
- Tapley, B. D., S. Bettadpur, M. Watkins, and C. Reigber (2004), The gravity recovery and climate experiment: Mission overview and early results, *Geophys. Res. Lett.*, *31*, L09607, doi:10.1029/2004GL019920.
- Tregoning, P., and C. Watson (2009), Atmospheric effects and spurious signals in GPS analyses, *J. Geophys. Res.*, doi:10.1029/2009JB006344, in press.
- Tregoning, P., G. Ramillien, and K. Lambeck (2008), GRACE estimates of sea surface height anomalies in the Gulf of Carpentaria, Australia, *Earth Planet. Sci. Lett.*, *271*, 241–244, doi:10.1016/j.epsl.2008.04.018.
- van Dam, T., J. Wahr, and D. Lavallée (2007), A comparison of annual vertical crustal displacements from GPS and Gravity Recovery and Climate Experiment (GRACE) over Europe, *J. Geophys. Res.*, *112*, B03404, doi:10.1029/2006JB004335.
- van der Wal, W., P. Wu, M. G. Sideris, and C. K. Shum (2008), Use of GRACE determined secular gravity rates for glacial isostatic adjustment studies in North America, *J. Geodyn.*, *46*, 144–154.
- Wahr, J., M. Molenaar, and F. Bryan (1998), Time-variability of the Earth’s gravity field: Hydrological and oceanic effects and their possible detection using GRACE, *J. Geophys. Res.*, *103*, 30,205–30,230.
- Wahr, J., D. Wingham, and C. Bentley (2000), A method of combining ICESat and GRACE satellite data to constrain Antarctic mass balance, *J. Geophys. Res.*, *105*, 16,279–16,294.

H. McQueen, P. Tregoning, and D. Zwartz, Research School of Earth Sciences, Australian National University, OHB-A, Building 61A, Mills Road, Canberra, ACT 0200, Australia. (paul.tregoning@anu.edu.au)

G. Ramillien, Dynamique Terrestre et Planétaire, UMR 5562, Observatoire, Midi-Pyrénées, Centre Nationale de la Recherche Scientifique, 14 avenue Edouard Belin, F-31400 Toulouse, France. (ramillie@legos.obs-mip.fr)